nature portfolio

https://doi.org/10.1038/s41560-021-00920-8

Supplementary information

Tailored catalyst microenvironments for CO_2 electroreduction to multicarbon products on copper using bilayer ionomer coatings

In the format provided by the authors and unedited

Supplementary Information

Tailored catalyst microenvironments for CO_2 electroreduction to multicarbon products on copper using bi-layer ionomer coatings

Chanyeon Kim[1,2,3], Justin C. Bui[1,2,3], Xiaoyan Luo[4], Jason K. Cooper[2,3], Ahmet Kusoglu[4], Adam Z. Weber[2,4] and Alexis T. Bell[1,2,3]*

[1]Department of Chemical and Biomolecular Engineering, University of California, Berkeley, California 94720.

[2]Liquid Sunlight Alliance, Lawrence Berkeley National Laboratory, Berkeley, California 94720.

[3]Chemical Sciences Division, Lawrence Berkeley National Laboratory, Berkeley, California 94720.

[4]Energy Technologies Area, Lawrence Berkeley National Laboratory, Berkeley, California 94720.

*Correspondence to: alexbell@berkeley.edu (A.T. Bell)

Supplementary Note 1: Calculation of CO_2 Mass Flux

I. Mass Transport in a Purely Aqueous System

For a given CO_2RR current density the mass flux of CO_2 at the Cu surface due to kinetics can be calculated as the following,

$$N_{CO_2,kinetic} = \frac{i_{CO_2RR}\left(\frac{n_{CO_2}}{n_{e^-}}|_{avg}\right)}{F} \quad (1)$$

where i_{CO_2RR} is the measured CO_2 reduction current density, F is Faraday's constant, and $\frac{n_{CO_2}}{n_{e^-}}|_{avg}$ is the average molar ratio of CO_2 to electrons for the surface reactions on Cu. Following prior work[1], this ratio was found to be 0.13. It is important to note that this Fick's Law expression assumes no interactions with the OH^-, but should be sufficient for the low current densities observed in this study[2]. Therefore, for a CO_2RR current density of 10 mA cm^{-2}, the flux of CO_2 at the surface is given as

$$N_{CO_2,kinetic} = \frac{10\ mA\ cm^{-2}\left(0.13\frac{mol\ CO_2}{mol\ e^-}\right)}{96485\frac{C}{mol\ e^-}} = 1.34\ x\ 10^{-4}\ mol\ m^{-2}\ s^{-1} \quad (2)$$

The mass transfer flux of CO_2 is given by

$$N_{CO_2,MT} = D_{CO_2,w}\frac{dc_{CO_2}}{dx} \quad (3)$$

where $D_{CO_2,w}$ is the diffusivity of CO_2 in aqueous solution (1.91 x 10^{-9} m^2 s^{-1})[3], and c_{CO_2} is the concentration of CO_2. The minimum mass-transport driven flux in a mass-transport limited scenario will be in the case where there is a linear profile between the Cu surface and the outer edge of the mass-transport boundary layer:

$$N_{CO_2,MT,min} = D_{CO_2,w}\frac{\Delta c_{CO_2}}{\Delta x} = (1.91\ x\ 10^{-9}\ m^2 s^{-1})\frac{34\ mM}{L_{BL}=100\ \mu m} \quad (4)$$

$$= 6.45\ x\ 10^{-4}\ mol\ m^{-2}\ s^{-1}$$

Because the minimum mass-transport limited flux through diffusion is larger than the kinetic flux of CO_2 at 10 mA cm^{-2}, it is very unlikely that there is a mass-transport limitation at this applied current

density.

II. Mass Transport with Ionomer Layers

For mass transport in the presence of the ionomer film, the kinetic mass flux stays the same, but the ionomer film modifies the diffusivity of CO_2 locally at the surface and modifies the mass transport driven flux. Again, assuming the limiting case of linear concentration profiles within the electrolyte and the ionomer layer, the following mass balance can be written at the ionomer/electrolyte interface:

$$N_{CO_2,MT,min} = D_{CO_2,w}\frac{\Delta c_{CO_2,2}}{\Delta x_2} = D_{CO_2,M}\frac{\Delta c_{CO_2,1}}{\Delta x_1} \quad (5)$$

where $D_{CO_2,w}$ is the diffusivity of CO_2 in the aqueous phase (1.91 x 10^{-9} m^2 s^{-1}), Δx_2 is the hydrodynamic boundary layer thickness (100 μm)[4], $\Delta c_{CO_2,2}$ is the change in CO_2 concentration within the aqueous phase given below,

$$\Delta c_{CO_2,2} = 34\ \text{mM} - \mathrm{c}_{\mathrm{CO}_2,ionomer|electrolyte}, \quad (6)$$

where $\mathrm{c}_{\mathrm{CO}_2,ionomer|electrolyte}$ is the concentration of CO_2 at the ionomer, electrolyte interface. 34 mM is the concentration of CO_2 in the bulk electrolyte.

$D_{CO_2,M}$ is the diffusivity of CO_2 in the ionomer phase, Δx_1 is the thickness of the ionomer, and $\Delta c_{CO_2,1}$ is the change in CO_2 concentration within the ionomer given below,

$$\Delta c_{CO_2,1} = \mathrm{c}_{\mathrm{CO}_2,ionomer|electrolyte} - c_{CO_2,Cu} \quad (7)$$

The diffusivity in the ionomer phase is given by

$$D_{CO_2,M} = \frac{\kappa_{CO_2,M}}{S_{CO_2,M}} \quad (8)$$

where $\kappa_{CO_2,M}$ is the permeability of CO_2 in the ionomer, and $S_{CO_2,M}$ is the solubility of CO_2 in the ionomer. Values for Δx_1 and $D_{CO_2,M}$ of the Nafion and Sustainion ionomers used in this study are shown in the following table.

Supplementary Table 1 | Used values for Δx_1 and $D_{CO_2,M}$ of the Nafion and Sustainion ionomers

Ionomer	Δx_1 (nm)	$D_{CO_2,M}$ (m^2 s^{-1})
Nafion	30	2.4 x 10^{-10}
Sustainion	40	3.57 x 10^{-12}

Further, for a mass-transport-limited scenario, the concentration at the electrode surface would have to be 0 mM, therefore,

$$c_{CO_2,Cu} = 0 \text{ mM} \tag{9}$$

Solving equation 8, $c_{CO_2,ionomer|electrolyte}$ for the various ionomers can be calculated, as well as the mass flux, $N_{CO_2,MT,min}$.

$$c_{CO_2,ionomer|electrolyte} = \frac{D_{CO_2,w}}{D_{CO_2,M}} \frac{\Delta x_1}{\Delta x_2} \frac{34 \text{ mM}}{(1+\frac{D_{CO_2,w}\Delta x_1}{D_{CO_2,M}\Delta x_2})} \tag{10}$$

$$N_{CO_2,MT,min} = \frac{D_{CO_2,w}}{\Delta x_2} \frac{34 \text{ mM}}{(1+\frac{D_{CO_2,w}\Delta x_1}{D_{CO_2,M}\Delta x_2})} \tag{11}$$

Supplementary Table 2 | Calculated values of $\Delta c_{CO_2,1}$, and $\Delta c_{CO_2,2}$ for the Nafion and Sustainion ionomers

Ionomer	$\Delta c_{CO_2,1}$ (mM)	$\Delta c_{CO_2,2}$ (mM)	$N_{CO_2,MT,min}$(mol m^{-2} s^{-1})
Nafion	0.08	33.92	6.4 x 10^{-4}
Sustainion	5.99	28.01	5.4 x 10^{-4}

Similarly, for the aqueous case, because the minimum mass-transport limited flux through diffusion is larger than the kinetic flux of CO_2 at 10 mA cm^{-2}, it is very unlikely that there is a mass-transport limitation at this applied current density.

Supplementary Note 2: Calculation of Ohmic Drop through Nafion and Sustainion Thin Films

The ohmic drop through a given ionomer layer can be calculated as follows,

$$V_{IR} = \frac{i_{total}}{\sigma_{ionomer}} \delta \quad (12)$$

where i_{total} is the total current density, $\sigma_{ionomer}$ is the conductivity of the ionomer, and δ is the ionomer thickness. Using this formula and assuming a total current density of 10 mA cm^{-2}, the following table can be evaluated for the ohmic drop in the relevant ionomers for this study.

Supplementary Table 3 | Calculation of ohmic drop due to ionic conductivity of ionomers

Ionomer	δ (nm)	$\sigma_{ionomer}$ (mS cm^{-1})	V_{IR} (μV)
Cs^+ form Nafion	30	20, Ref. [5]	1.5
HCO_3^- form Sustainion	40	24, Ref. [6]	1.67
OH^- form Sustainion	40	64, Ref. [6]	0.63

Supplementary Note 3: Optimum loading amount of ionomer

As shown in Supplementary Fig 2, in the case of Nafion-coated Cu (Naf 1100/Cu, Nafion with 1100g mol^{-1} of EW), while the total current densities showed only a slight decline in the range from –15 to –13.5mA cm^{-2}, the product distribution varied considerably with Nafion loading. The FE for H_2 decreased from 20 to 9 % with increased Nafion loading amount up to 6μg cm^{-2} and then increased slightly to 12% with further increase in Nafion loading up to18 μg cm^{-2}. Since increasing the Nafion loading to 6μg cm^{-2} noticeably increased the FE to C_{2+} products, all further work on the effects of Nafion was performed with a loading of 6μg cm^{-2}. While the Nafion thin film on Cu produced only marginal changes in the total current density for samples prepared with different loadings, similar experiments with Sustainion demonstrated a significant increase in the total current density with increasing ionomer loading, from –15mA cm^{-2} for bare Cu to –24mA cm^{-2} for Cu with the 18μg cm^{-2} of Sustainion. However, Cu with the 18 μg/cm^2 of Sustainion also exhibited the highest FE to the HER. Further investigations of the Sustainion layer were conducted with a loading of 6μg cm^{-2}, which exhibited the lowest FE to the HER but still achieved a total current density of –22mA cm^{-2}.

The existence of an optimum loading is likely due to changes in microenvironment with the addition of more Nafion or Sustainion. As shown in above in **Table 1**, both Nafion and Sustainion exhibit larger CO_2/H_2O ratios than pure aqueous solution, which would lead to an enhancement of C_{2+} current density for both cases. Interestingly, as the loading is increased, ethylene is suppressed at the expense of ethanol formation. This shift in the selectivity from fully saturated to partially saturated products has been attributed to a relative increase in the concentration of adsorbed *CO when compared to *H on the surface of Cu[7]. The ratio of *CO to *H should correlate to the ratio of CO_2/H_2O and supports the hypothesis that the ratio of CO_2/H_2O can be used to predict C_{2+} selectivity. However, as the ionomer loading increases, the CO_2R selectivity decreases at the expense of H_2 formation, likely due to CO_2 mass transport limitations incurred when operating with a thicker film.

Supplementary Note 4: Calculation of Dynamic and Static FE

For clear comparison with static electrolysis of CO_2R using bare Cu, the mean value of the FE for bare Cu was calculated using the following equation.

$$FE_{mean,i} = \frac{j_{-1.15V} \times FE_{-1.15\ ,i} + j_{-0.8V} \times FE_{-0.8V,i}}{j_{-1.15V} + j_{-0.8V}} \quad (13)$$

In this equation, $j_{-0.8V}$ and $j_{-1.15V}$ are current densities measured for static electrolysis at –0.80 and –1.15 V vs RHE, and $FE_{-0.8V,i}$ and $FE_{-1.15V,i}$ are the faradaic efficiencies for product i measured for static electrolysis at –0.8 and –1.15 V vs RHE.

Supplementary Note 5: Electrochemical reduction of acetonitrile

As shown in Supplementary Fig 11, the effect of ionomer on the local pH near the surface of Cu was confirmed by conducting the electrochemical reduction of acetonitrile to ethylamine. A recent report of this reaction over a Cu catalyst demonstrated that the selectivity to ethylamine was improved by suppressing HER by switching the electrolyte from Na_2SO_4 to NaOH, since HER is pH-sensitive but the formation of ethylamine is not[8]. To investigate the effect of ionomer on HER in the environment of electrochemical acetonitrile reduction, LSV was conducted using Cu, Naf850/Cu, Sus/Cu, and Naf850/Sus/Cu. The total current density measured during LSV from -0.4 V to -0.8 V increased in the order of Naf850/Sus/Cu < Naf850/Cu < Cu < Sus/Cu, corresponding to the increase in the rate of the HER in the same order as confirmed by DEMS. On the other hand, the rate of ethylamine formation over the tested Cu catalysts was similar due to the insensitivity of this reaction to the electrolyte pH. These results imply that the ionomer in the outermost layer can alter the local pH, where Nafion enhances accumulation of OH^- generated during electrochemical acetonitrile reduction due to the Donnan exclusion while Sustainion enhances transport of OH^- from the Cu surface to the bulk electrolyte.

Supplementary Note 6: Analysis using differential electrochemical mass spectroscopy

As shown in Supplementary Fig 13, another interesting characteristic of H_2, CH_4, and C_{2+} formation over ionomer-coated Cu catalysts was observed by differential electrochemical mass spectroscopy (DEMS). DEMS enables the observation of the transient evolution of each product near the Cu surface with a 0.5 s time resolution response to the stimulus of the system (i.e. applied potential). Since both HER and CO_2RR generate OH^-, a more cathodic applied potential would result in higher local pH. Thus, the local pH in the microenvironment of Cu could differ between cathodic and anodic potential sweeps. In this regard, the formation of H_2, CH_4 and C_2H_4 during cyclic voltammetry were monitored by DEMS. While Sus/Naf 850/Cu and Sus/Cu showed a significant increase in both H_2 and CH_4 formation during anodic sweeps (from more cathodic to less cathodic potential), Naf 850/Sus/Cu, Naf 850/Cu and bare Cu showed significant decreases in H_2 formation and only slight decreases in CH_4 formation during the anodic sweep. On the other hand, all tested Cu catalysts showed increases in C_2H_4 formation during the anodic sweep. These results can be rationalized by transient changes in local pH and the replenishment of local CO_2 during the anodic scan. For Naf 850/Sus/Cu, Naf 850/Cu and bare Cu, the higher local pH formed at the more cathodic potential would decrease H_2 and CH_4 formation but the replenished local CO_2 during the anodic scan would increase CH_4 and C_2H_4 formation offsetting the decrease in CH_4 formation. On the other hand, for Sus/Naf 850/Cu and Sus/Cu, the lower local pH and replenished local CO_2 would result in increased formation of H_2, CH_4 and C_2H_4.

Supplementary Figures

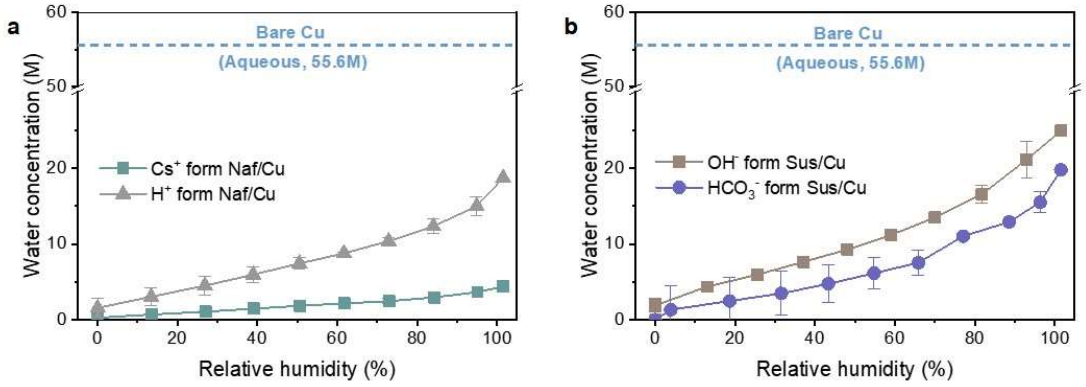

Supplementary Fig. 1 | Measurement of ionomer thin-film on Cu with different counter-ions. Blue dashed line indicates water concentration of aqueous solution corresponding to bare.

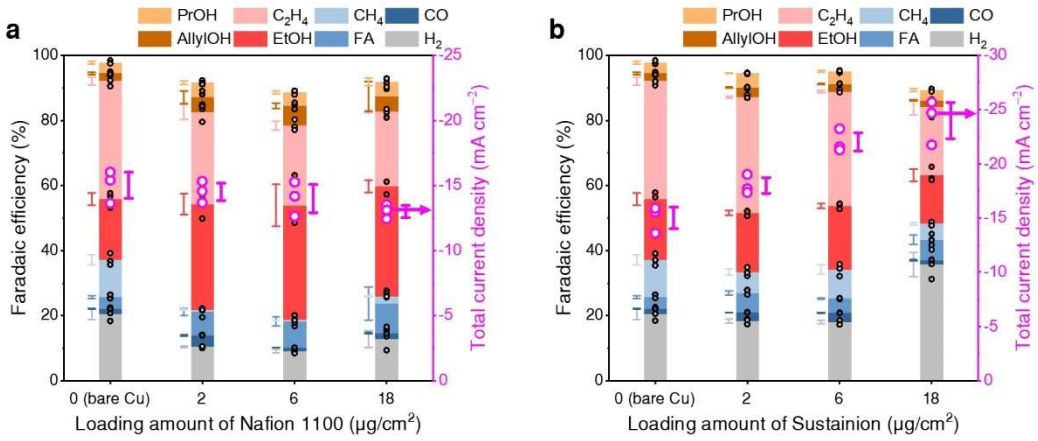

Supplementary Fig. 2 | Optimization of loading amount of ionomer. CO_2R performance of **a,** Nafion (with 1100 g mol^{-1} of EW) and **b,** Sustainion coated Cu. Catalytic performance was evaluated using 0.1M $CsHCO_3$ electrolyte at -1.15 V vs RHE, where bare Cu showed the best catalytic performance in terms of C_{2+} production. In **a** and **b**, Error bars indicate standard deviation among values from 3 repeated measurements.

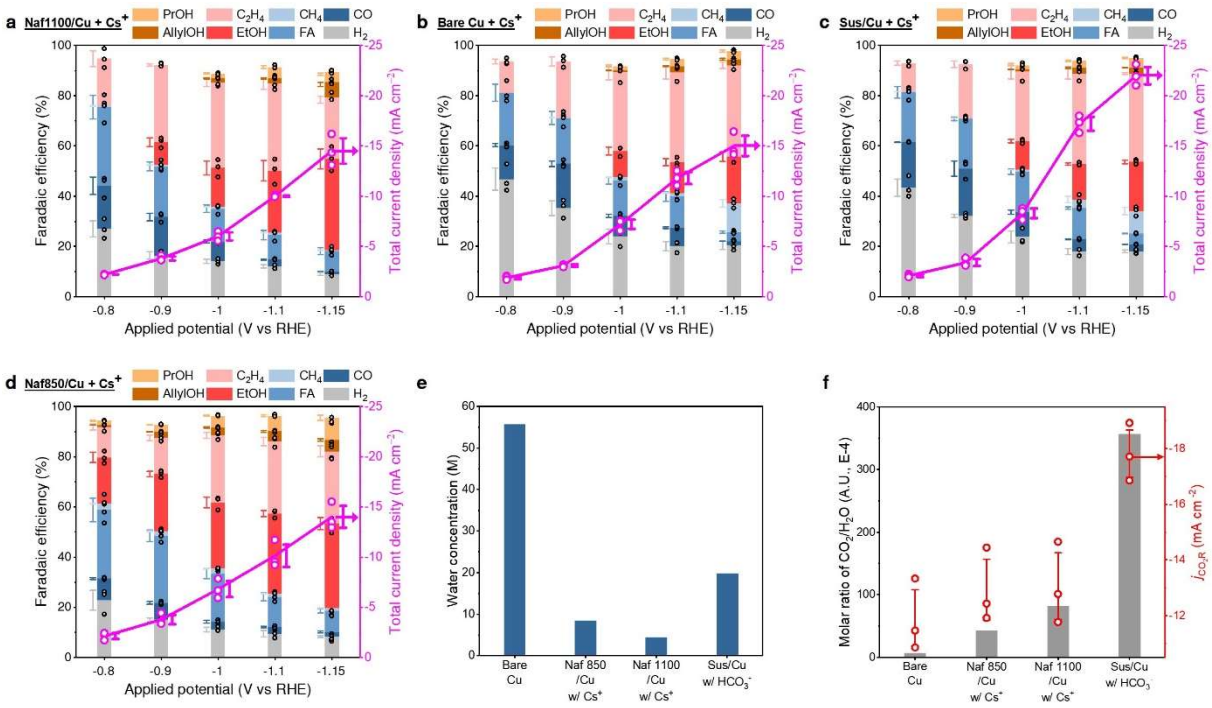

Supplementary Fig. 3 | CO_2R using ionomer-coated Cu. Catalytic performance of CO_2R using **a** Naf1100/Cu, **b** bare Cu, **c** Sus/Cu, and **d** Naf850/Cu in the presence of 0.1M $CsHCO_3$ electrolyte. **e,** Measurement of water concentration for ionomer-coated Cu at 100% relative humidity; each sample was ion-exchanged using 0.1M $CsHCO_3$ electrolyte prior to the measurement. **f,** Estimation of local CO_2/H_2O based on measured water concentration in **g** and corresponding partial current densities at -1.15V vs RHE (open symbols). In **a**-**d** and **f**, Error bars indicate standard deviation among values from 3 repeated measurements which are plotted as dots.

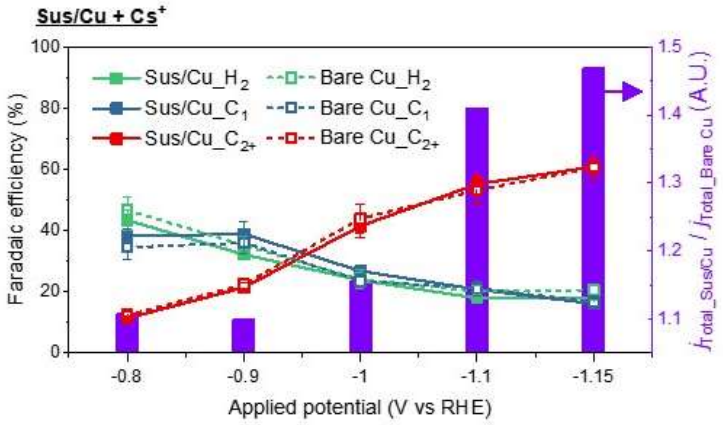

Supplementary Fig. 4 | Comparison of CO_2R performance between Sustainion-coated Cu (Sus/Cu) and bare Cu. Catalytic performance was evaluated using 0.1M $CsHCO_3$ electrolyte at -1.15 V vs RHE. Sus/Cu showed very similar product distribution to that obtained from bare Cu which noted as colored symbol and line, but considerably increased total current density compared to that obtained from bare Cu, which is noted as purple column. Error bars indicate standard deviation among values from 3 repeated measurements.

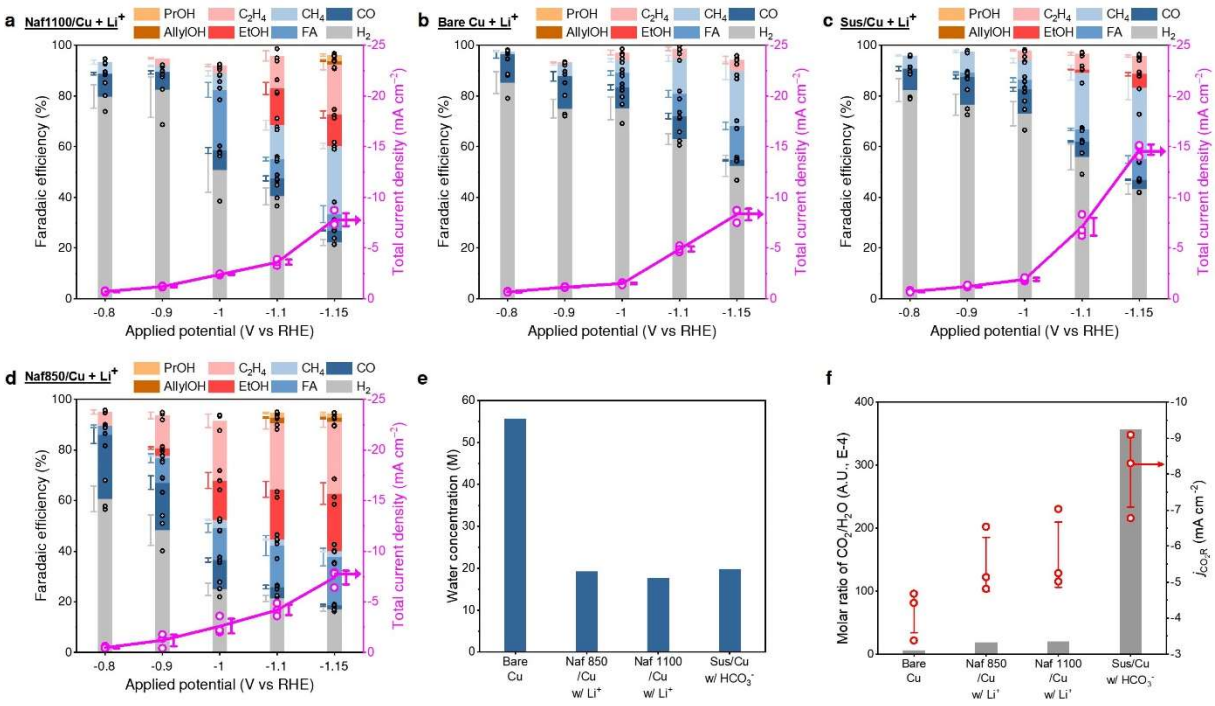

Supplementary Fig. 5 | Effect of cation identity on CO_2R using ionomer-coated Cu. Catalytic performance of CO_2R using **a** Naf1100/Cu, **b** bare Cu, **c** Sus/Cu, and **d** Naf850/Cu in the presence of 0.1M $LiHCO_3$ electrolyte. **e**, Measurement of water concentration for ionomer-coated Cu at 100% relative humidity; each sample was ion-exchanged using 0.1M $LiHCO_3$ electrolyte prior to the measurement. **f**, Estimation of local molar ratio between CO_2 and H_2O and corresponding partial current densities at –1.15V vs RHE (open symbols). In **a-d** and **f**, Error bars indicate standard deviation among values from 3 repeated measurements which are plotted as dots.

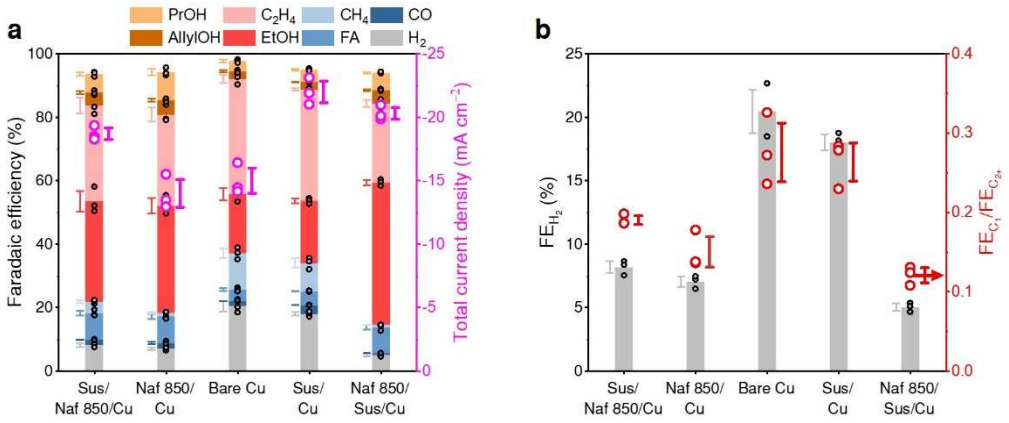

Supplementary Fig. 6 | Effect of stacking ionomer layers. a, CO_2R performance at –1.15V vs RHE using stacked ionomers on Cu in the presence of 0.1M $CsHCO_3$ electrolyte. **b**, Trend in H_2, C_1, and C_{2+} formation for ionomer-coated Cu tested in **a**. It is noted that the ratio of FE for C_1 and that C_{2+} in the right axis of **b** is dimensionless. In **a** and **b**, Error bars indicate standard deviation among values from 3 repeated measurements which are plotted as dots.

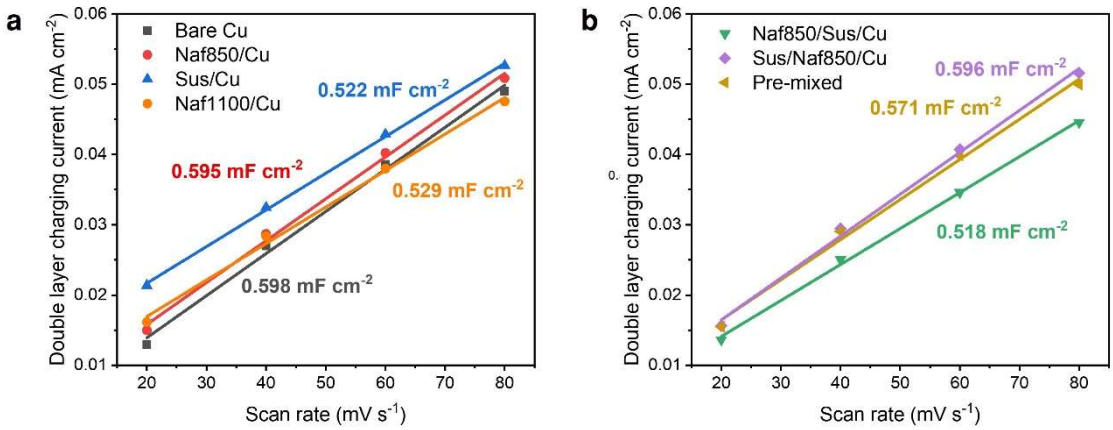

Supplementary Fig. 7 | Estimation of the electrochemical surface area (ECSA) for ionomer coated Cu by measurement of double layer charging current at different scan rate of potential. Measured double layer charging current for **a** bare Cu, Naf850/Cu, Naf1100/Cu, and Sus/Cu. and for **b** Naf850/Sus/Cu, Sus/Naf850/Cu, and Pre-mixed Nafion and Sustainion on Cu (Pre-mixed/Cu).

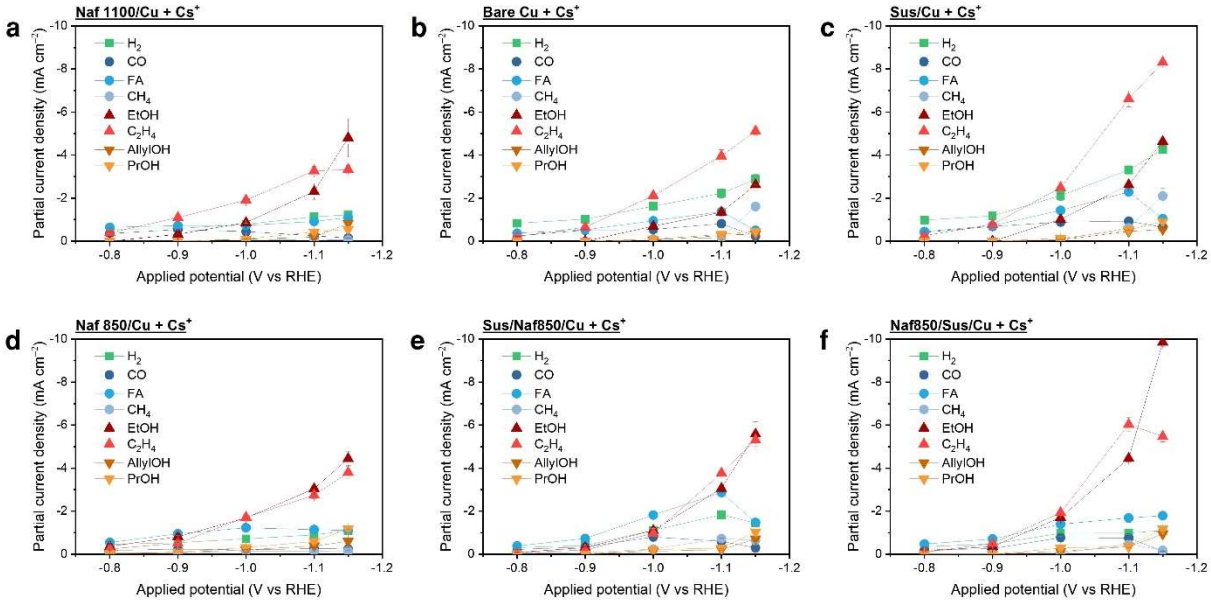

Supplementary Fig. 8 | ECSA normalized partial current density during CO_2R on ionomer coated Cu. Normalized partial current density using 0.561 mF cm^{-2} of averaged ECSA for **a** Naf11000/Cu, **b** Bare Cu, **c** Sus/Cu, **d** Naf850/Cu, **e** Sus/Naf850/Cu, and **f** Naf850/Sus/Cu.

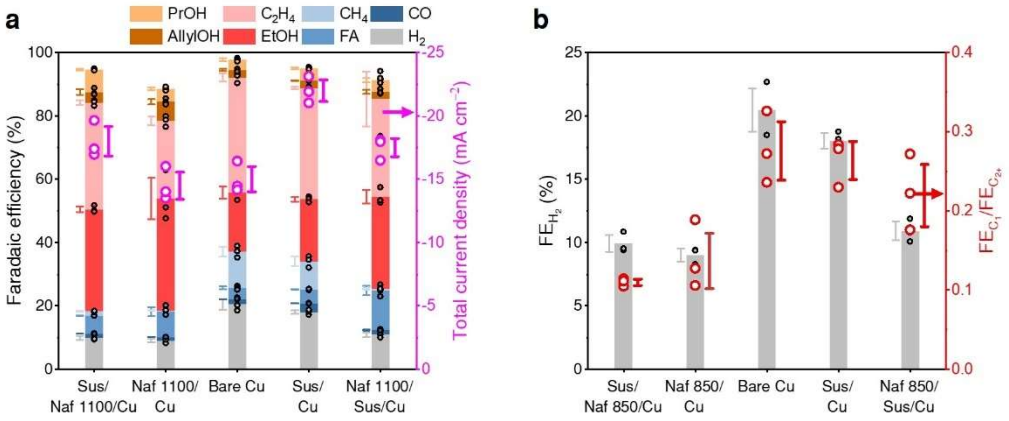

Supplementary Fig. 9 | Effect of stacking Nafion with 1100g mol_{eq}^{-1} and Sustainion layers. a, CO_2R performance at −1.15 V vs RHE using stacked ionomers on Cu in the presence of 0.1M $CsHCO_3$ electrolyte. **b,** Trend in H_2, C_1, and C_{2+} formation for ionomer coated Cu tested in **a**. In **a** and **b**, Error bars indicate standard deviation among values from 3 repeated measurements which are plotted as dots.

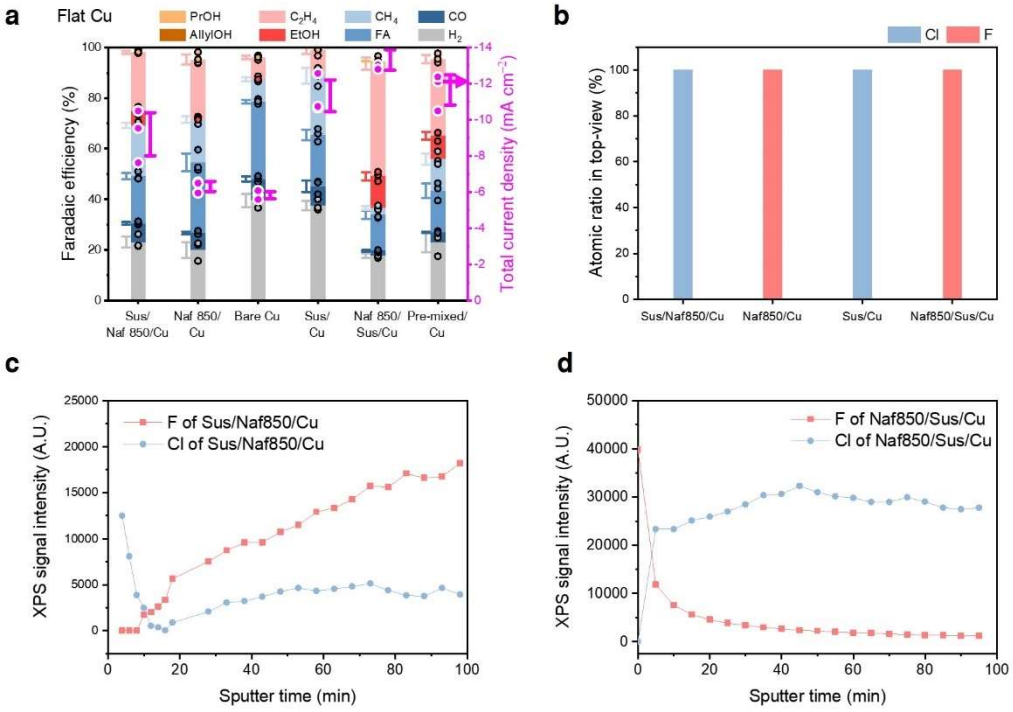

Supplementary Fig. 10 | Effect of configuration of ionomer layers. a, CO_2R performance at –1.15V vs RHE using ionomer coatings on flat Cu surface (Cu/Si wafer). Error bars indicate standard deviation among values from 3 repeated measurements which are plotted as dots. XPS analysis on ionomer coated flat Cu surface **b,** on top-view, and **c-d,** in-depth using Ar sputtering.

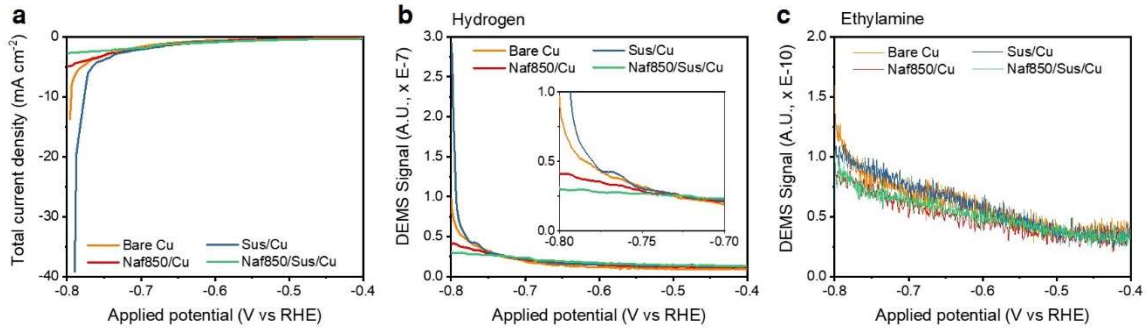

Supplementary Fig. 11 | Effect of ionomer on electrochemical reduction of acetonitrile to ethylamine. a, linear sweep voltammetry (LSV) of ionomer coated Cu in the presence of nitrogen purged (20 sccm) 0.5M Na_2SO_4 electrolyte with 8 wt% of acetonitrile. Temporal evolution of **b,** H_2 and **c**, ethylamine monitored by DEMS. LSV was conducted with 1 mV s^{-1} of sweep rate.

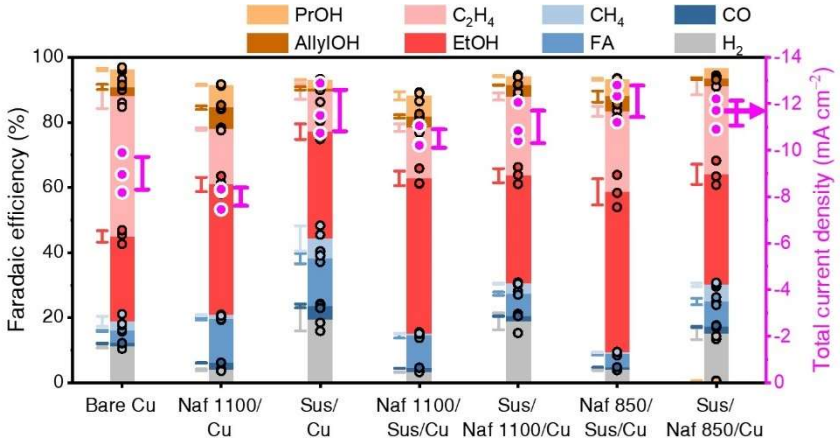

Supplementary Fig. 12 | Synergy between microenvironment using ionomer layers and pulsed CO_2 electrolysis. Faradaic efficiencies of pulsed CO_2 electrolysis using various ionomer-coated Cu catalysts. Pulsed electrolysis was conducted using a square-wave potential pulse consisting of 10s of duration at –1.15 and –0.8 V vs RHE each. Error bars indicate standard deviation among values from 3 repeated measurements which are plotted as dots.

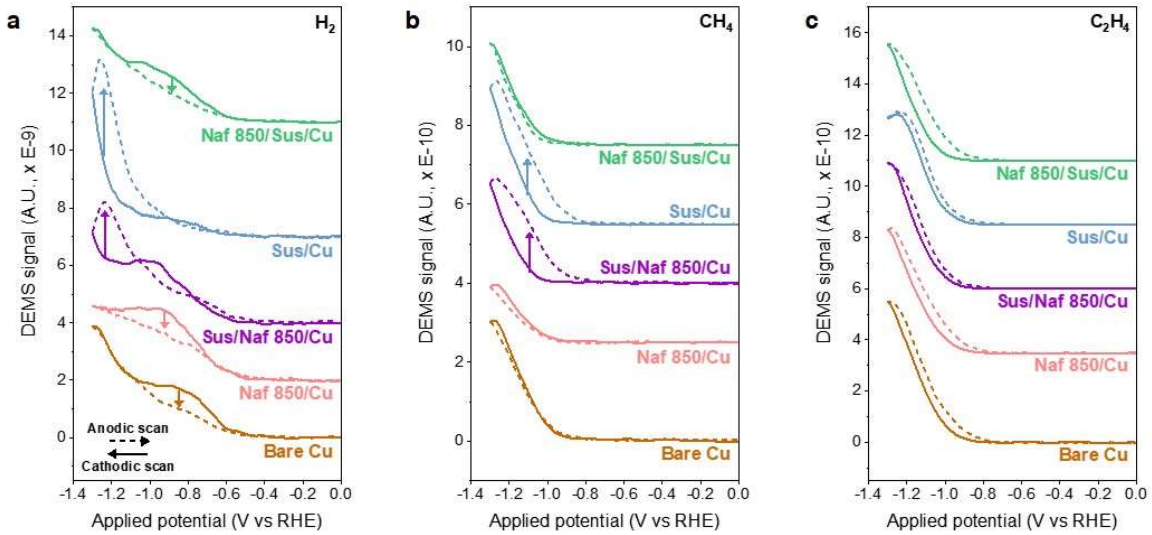

Supplementary Fig. 13 | Differential electrochemical mass spectra (DEMS) during cyclovoltammetry using various Cu catalysts with or without ionomer layers. DEMS used for observation of temporal evolution of **a,** H_2, **b,** CH_4, **c,** C_2H_4. Cyclovoltammetry was conducted in the range of 0 to −1.3 V vs RHE with 10mV s^{-1} of sweep rate. Each solid line and dotted line indicate DEMS profile during cathodic (0 to −1.3 V vs RHE) and anodic (−1.3 V to 0V vs RHE) scan, respectively.

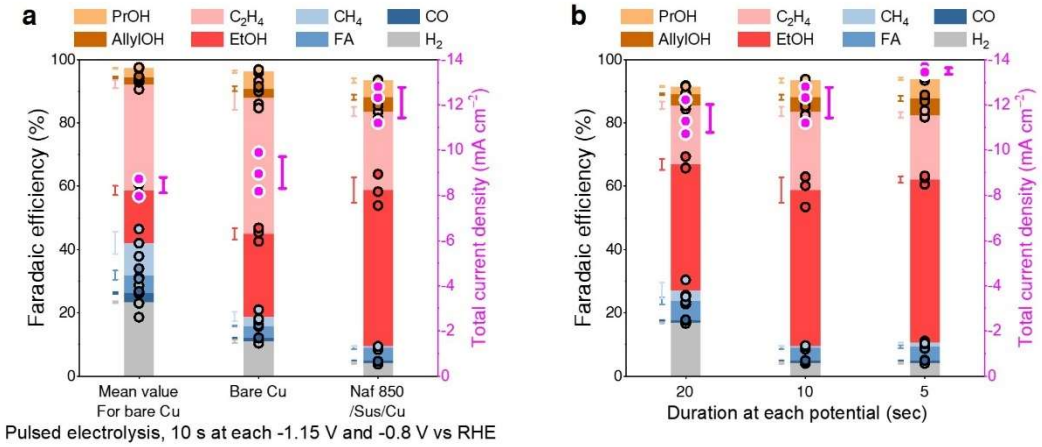

Supplementary Fig. 14 | Comparison of pulsed CO_2RR performance. a, Comparison among mean value, bare Cu and Naf 850/Sus/Cu and **b,** Comparison between pulsed electrolysis using Naf 850/Sus/Cu with different duration at each potential. In **a,** the mean value was calculated from catalytic performance obtained during static electrolysis at -1.15V and -0.8V vs RHE using bare Cu which represents control group without any effects from ionomer layer nor pulsed electrolysis. In **a** and **b**, Error bars indicate standard deviation among values from 3 repeated measurements which are plotted as dots.

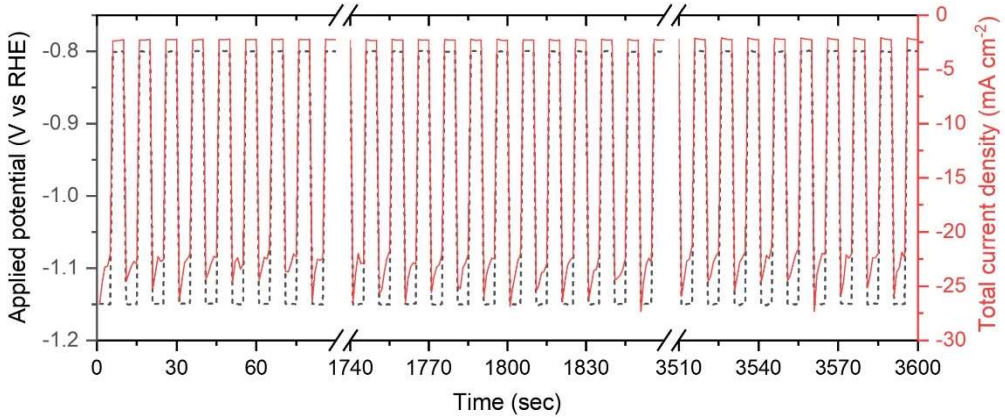

Supplementary Fig. 15 | Pulsed electrolysis with the optimal duration at each potential. Black dotted line indicates applied potential pulse with respect to the time and red solid line indicates measured total current density during the pulsed electrolysis.

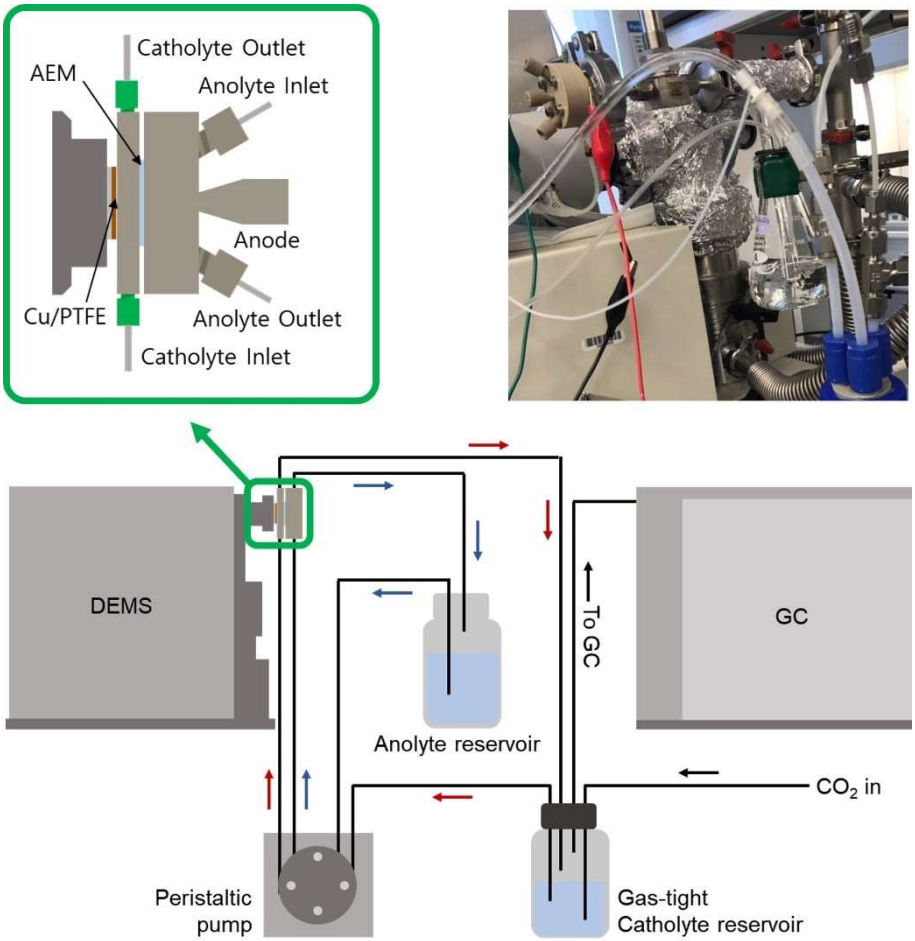

Supplementary Fig. 16 | Experimental setup enabling analysis of both local and bulk composition of products during CO_2R.

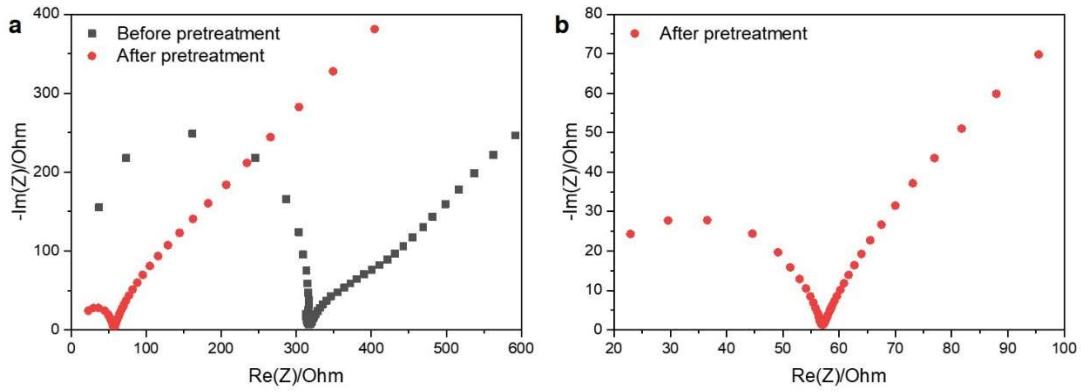

Supplementary Fig. 17 | Activation of Sustainion/Cu after 30 min of chronoamperometry at -0.7 V vs RHE. Impedance diagram of **a,** Sustainion/Cu with or without activation and **b,** magnified area for activated sample. Pristine Sustainion ionomer cast Cu showed significantly large hemi circle in impedance diagram as noted as black dots due to chloride counter anion. Then, Sus/Cu can be activated after 30 min of chronoamperometry at -0.7V vs RHE, significantly reduced hemi circle in impedance diagram as noted as red dots indicating Sustainion layer was ion-exchanged from chloride anion to bicarbonate anion. It is also noted that all the tested Cu catalysts with or without ionomer showed similar uncompensated resistance around 60 Ω.

Supplementary References

1. C. Kim, L.-C. Weng, A. T. Bell, Impact of Pulsed Electrochemical Reduction of CO_2 on the Formation of C_{2+} Products over Cu. *ACS Catal.* **10**, 12403-12413 (2020).
2. H. Hashiba *et al.*, Effects of Electrolyte Buffer Capacity on Surface Reactant Species and the Reaction Rate of CO_2 in Electrochemical CO_2 Reduction. *J. Phys. Chem. C* **122**, 3719-3726 (2018).
3. R. E. Zeebe, On the molecular diffusion coefficients of dissolved CO_2,HCO_3^-, and CO_3^{2-} and their dependence on isotopic mass. *Geochim. Cosmochim. Acta* **75**, 2483-2498 (2011).
4. J. C. Bui, C. Kim, A. Z. Weber, A. T. Bell, Dynamic Boundary Layer Simulation of Pulsed CO_2 Electrolysis on a Copper Catalyst. *ACS Energy Lett.*, 1181-1188 (2021).
5. A. R. Crothers, R. M. Darling, A. Kusoglu, C. J. Radke, A. Z. Weber, Theory of Multicomponent Phenomena in Cation-Exchange Membranes: Part II. Transport Model and Validation. *J. Electrochem. Soc.* **167**, 013548 (2020).
6. Z. Liu, H. Yang, R. Kutz, R. I. Masel, CO_2 Electrolysis to CO and O_2 at High Selectivity, Stability and Efficiency Using Sustainion Membranes. *J. Electrochem. Soc.* **165**, J3371-J3377 (2018).
7. J. Li *et al.*, Constraining CO coverage on copper promotes high-efficiency ethylene electroproduction. *Nat. Catal.* **2**, 1124-1131 (2019).
8. R. Xia *et al.*, Electrochemical reduction of acetonitrile to ethylamine. *Nat. Commun.* **12**, 1949 (2021).